The predictability of the downward vs. non-downward propagation of sudden stratospheric warmings in S2S hindcasts

David M. Nebel[1,2], Chaim I. Garfinkel[1], Judah Cohen[3,4], Daniela I.V. Domeisen[5,2], Jian Rao[6], Chen Schwartz[1,7]

[1]Fredy and Nadine Herrmann Institute of Earth Sciences, Hebrew University, Jerusalem, Israel
[2]Institute for Atmospheric and Climate Science, ETH Zurich, Zurich, Switzerland
[3]Atmospheric and Environmental Research Inc., Lexington, MA, USA.
[4]Massachusetts Institute of Technology, Cambridge, MA, USA
[5]University of Lausanne, Lausanne, Switzerland
[6]Key Laboratory of Meteorological Disaster, Ministry of Education (KLME), Joint International Research Laboratory of Climate and Environment Change (ILCEC), Collaborative Innovation Center on Forecast and Evaluation of Meteorological Disasters (CIC-FEMD), Nanjing University of Information Science and Technology, Nanjing 210044, China
[7]Centre for Climate Research Singapore, Singapore

Key Points:

- Downward impact of anomalies after SSWs is evaluated for 7 subseasonal prediction models for 16 events.
- Models predict downward propagation to 100hPa two weeks before SSW onset, though they struggle for impacts in the troposphere.
- Downward impact and predictability of SSWs unrelated; split and absorbing SSWs show stronger downward impact in models and reanalysis

Corresponding author: Chaim I. Garfinkel, `chaim.garfinkel@mail.huji.ac.il`

Abstract

Roughly one-third of sudden stratospheric warming (SSW) events lack a strong canonical surface impact, and this can lead to a forecast bust if a strong impact had been predicted. Hence, it is important to predict before the SSW onset if an event will propagate downward. The predictability of the downward impact of SSWs is considered in 7 subseasonal-to-seasonal forecast models for 16 major SSWs between 1998 and 2022, a larger sample size than considered by previous works. The models successfully predict which SSWs have a stronger downward impact to 100hPa, however they struggle to predict which have a stronger tropospheric impact. The downward impact is stronger if the deceleration of the 10hPa winds is better predicted. Downward impact is stronger for split and for absorbing SSWs, and is better predicted in high-top models. In contrast, there is little relationship between SSWs with above-average predictability and the subsequent downward impact.

Plain Language Summary

The wintertime stratosphere typically features circumpolar strong westerly winds, but on occasion these strong winds can reverse and temperatures over the pole can rise by tens of degrees in an event known as a sudden stratospheric warming (SSW). Such an event is typically followed by extreme cold over Northern Eurasia and wet conditions in Southern Europe, however roughly a third of events do not feature such downward propagation. Sixteen SSW events have occurred in the Northern Hemisphere over the period 1998 to 2022, and this study considers whether the models that have contributed re-forecasts and real-time forecasts to the subseasonal to seasonal (S2S) database archive are able to distinguish which are downward propagating and which are not. We also explore the factors that govern downward propagation of the SSW signal in these models.

1 Introduction

Sudden stratospheric warmings (SSW) are among the most extreme phenomena in the climate system. During a major SSW event, temperatures in the polar mid-stratosphere increase by tens of kelvins and the circumpolar westerly winds reverse to easterly winds, associated with decelerations of several tens of meters per second (Schoeberl, 1978; Charlton & Polvani, 2007; Butler et al., 2015; Baldwin et al., 2021). During the occurrence of Northern Hemisphere (NH) SSW events, the Northern Annular Mode (NAM) in the stratosphere shifts toward its negative phase on average, and the negative NAM signal propagates downward in the following weeks and can then persist for up to a few months in the troposphere (Baldwin et al., 2003; Sigmond et al., 2013; Tripathi et al., 2015). Typical surface impacts include anomalous cold air outbreaks in the North Atlantic and northern Eurasia, anomalous warmth over Greenland and Eastern Canada, and an enhanced storm track and precipitation over Southern Europe and parts of East Asia (Thompson et al., 2002; Kolstad et al., 2010; Lehtonen & Karpechko, 2016; Garfinkel et al., 2017; Kretschmer et al., 2018; Karpechko et al., 2018; Afargan-Gerstman et al., 2020, 2024).

Not all SSWs are followed by the canonical persistent negative NAM in the troposphere, however. This divergence in the downward propagation leads to SSWs being classified as either downward propagating or non-downward propagating events (Black & McDaniel, 2004; Jucker, 2016; Runde et al., 2016; Kodera et al., 2016; Karpechko et al., 2017; I. White et al., 2019). Several potential factors have been proposed to help determine the (non)downward propagation of SSW events: the vortex geometry (i.e., displacement/split morphology), especially for the first few weeks after SSW onset (Mitchell et al., 2013; Maycock & Hitchcock, 2015; I. P. White et al., 2021); the strength of the upward wave forcing that precedes the SSW (I. White et al., 2019); the propagation of the initial circulation anomalies from the upper to the lower stratosphere and the subsequent strength and duration of lower stratospheric anomalies (Black & McDaniel, 2004; Hitchcock et al., 2013; Karpechko et al., 2017); absorption/reflection of planetary waves in the stratosphere following SSWs (Kodera et al., 2016), and preexisting tropospheric circulation conditions (Hitchcock & Simpson, 2014; Afargan-Gerstman & Domeisen, 2020; D. I. V. Domeisen, Grams, & Papritz, 2020). The lower stratosphere accounts for roughly 40% of the variance in surface impact, while tropospheric preconditioning also plays an important role (Afargan-Gerstman et al., 2022).

Subseasonal to seasonal (S2S) prediction models are generally able to capture the average downward response and surface impact arising from the stratospheric forcing (D. I. V. Domeisen, Butler, et al., 2020). Though since only roughly two-thirds of SSW events have a discernible surface impact, quite uniformly across definitions of such an impact (Karpechko et al., 2017; D. I. Domeisen, 2019), it is important for the models to capture which events specifically have a downward impact. When it comes to predicting the specific impact of particular events the models exhibit much lower skill, especially over Europe, where both sub-seasonal (D. I. V. Domeisen, Butler, et al., 2020) and seasonal (Kolstad et al., 2020) prediction models tend to be over-confident and often predict a surface response when there is none, or vice versa. As an example, the strong canonical surface impact of the 2018 SSW event was primarily captured by the sub-seasonal prediction model once the SSW event had occurred and propagated into the lower stratosphere (Rao et al., 2020; D. I. Domeisen et al., 2022). In general, the expected canonical surface response to SSWs that occurs in two-thirds of cases is significantly better predicted by the models than the unexpected non-canonical response (Afargan-Gerstman et al., 2024).

A prediction of a downward impact that subsequently does not verify can strongly impact extended forecast skill at the surface, leading to unwanted forecast busts. Hence, it is crucial to understand to what extent models are able to represent and predict the downward impact of specific events, and to identify possible reasons for the model behavior or biases, which will ultimately benefit the understanding of downward coupling from the stratosphere. We begin by considering whether S2S models are capable of dis-

tinguishing which SSWs will propagate downward. While previous work has considered the ability of models to capture downward propagation for particular events using real-time forecasts (Karpechko et al., 2018; Rao et al., 2020), downward impacts from SSWs in the hindcasts of S2S models have not been explored. Further, the difference in observed and simulated downward propagation among these events (as shown below) motivates the question: why is there spread across events in the magnitude of the downward impact of SSWs? We will also answer this question in this study.

2 Methods and Data

The Subseasonal-to-Seasonal (S2S) Prediction project (Vitart et al., 2017) has made available a large number of hindcasts covering the past several decades. Of the eleven modeling centers for which data was available when this study was initiated, we focus on seven models that include output to at least week six and which also output data at the 10hPa level. These modeling centers are: the Australian Bureau of Meteorology (BoM), the China Meteorological Administration (CMA), Météo-France (CNRM), the European Centre for Medium-Range Weather Forecasts (ECMWF), the National Center for Environmental Prediction (NCEP), the Korean Meteorological Agency (KMA), and the United Kingdom Met Office (UKMO). We downloaded hindcasts for the operational model in use during the winter of 2019/2020 for all models (for ECMWF, this is cycle CY46R1), except for (1) CNRM, which was upgraded later in 2020 and for which we use the model version from winter 2020/2021, and for (2) CMA, which upgraded in the middle of winter 2019/2020. (Further, the hindcasts of the newer CMA version begin only in 2004 and hence miss all SSWs from 1998 to 2003). For the ECMWF model, we downloaded only one hindcast each week, and for the NCEP model, we only downloaded 9 hindcasts each month, for consistency with the data availability from the rest of the models. ERA5 reanalysis is used as the atmospheric reference to which forecast systems are compared (Hersbach et al., 2020). These various models differ in the quality of their representation of the stratosphere: the stratosphere is less well resolved in BoM and the CMA version used here as compared to the other models.

Each modeling center has made available hindcasts from different years, and further, the initialization dates differ among the models even for a given year. It is therefore necessary to separately composite reanalysis data according to the actual initializations used for each model in order to meaningfully compare the modeled and observed responses. Anomalies of zonal wind at 10hPa, 60N (U1060) and polar cap height area-weighted from 70N to the pole at 500hPa and 100hPa (Zcap500 and Zcap100) for each model forecast are computed by comparing to a lead-time and initialization-date dependent climatology from the S2S hindcasts.

We focus on sixteen SSWs that have occurred since 1998, eleven of which occurred in the period common to all models (1999-2010). The onset dates we adopt for these SSWs are: 12-15-1998, 02-26-1999, 03-20-2000, 02-11-2001, 12-30-2001, 01-18-2003, 01-05-2004, 01-21-2006, 02-24-2007, 02-22-2008, 01-24-2009, 02-09-2010, 01-06-2013, 02-12-2018, 01-01-2019, and 01-05-2021. Note that the first day of easterly winds can differ among reanalysis products, however for these events modern reanalyses agree to within one day of each other (e.g. Butler et al., 2017), and hence these differences do not impact our results. We focus on the hindcast data for the thirteen SSW events that occurred between 1998 and 2013, and real-time forecasts for three SSWs in 2018, 2019, and 2021. At least four of the S2S systems are included for each event.

For each event, we also consider the possible contribution of the El Niño-Southern Oscillation (ENSO), Madden Julian Oscillation (MJO), and Quasi-Biennial Oscillation (QBO) to downward propagation. The ENSO state is characterized using the observed Niño3.4 index extracted from monthly mean ERSSTv5 data (Huang et al., 2017) for the calendar month which contains the onset date of the SSW. The QBO state is character-

ized using the observed zonal mean zonal wind at 50hPa in monthly mean NCEP CDAS reanalysis data for the calendar month which contains the day of the SSW. The MJO state is defined following Wheeler and Hendon (2004), and specifically we compute the average amplitude and phase using the two Real-time Multivariate MJO Indices from 5 to 15 days before the SSW in order to characterize the MJO state preceding a SSW (motivated by Garfinkel et al., 2012). If the amplitude is below 1.0, then the MJO is considered to be inactive. The characterization of a SSW as either split or displacement, and also the onset date of the event, follows Table 1 of Cohen and Jones (2011) for earlier events, Tripathi et al. (2016) for the 2013 event, and Rao et al. (2020) and Rao et al. (2021) for the three most recent events.

The categorization of SSW events into the "absorbing type" and the "reflecting type" is performed for each of two distinct methodologies. First, we use the criteria set forth by Messori et al. (2022). The reflection index (RI), as defined by Messori et al. (2022), is equal to the difference in anomalous poleward eddy heat fluxes at 100 hPa between Siberia (Sib) and Canada (Can): $RI = \overline{v'T'}_{Sib} - \overline{v'T'}_{Can}$. Here, v represents the meridional wind speed and T signifies the temperature. The prime symbols represent deviations from the zonal mean. Weighted averages are determined over Siberia (Sib; between 45-75°N and 140-200°E) and Canada (Can; between 45-75°N and 230-280°E). The regional time series data has been standardized by subtracting the daily mean and then dividing by the daily standard deviation. Reflection events are then defined as days when the RI value surpasses 1 for a minimum of 10 consecutive days. Lastly, the 15-day period following each SSW was examined to determine whether a reflection event had occurred during that time. If a SSW was followed by a reflection event within this 15-day window, it was categorized accordingly. If not, it was labeled under the category of "absorbing". Classifying the SSWs in this way results in the following SSWs being characterized as absorbing: 1998-12-15, 1999-02-25, 2000-03-20, 2009-01-24, 2018-02-12, and 2021-01-05. (Note that the 2021-01-05 event was absorbing in most of January, though it transitioned to reflecting later, Cohen et al., 2021). The other ten are "reflecting". The second methodology follows the definition of reflecting and absorbing from Kodera et al. (2016) and Karpechko et al. (2017), who instead focus on negative planetary wave heat flux at 100hPa. We have reproduced the list of events from Karpechko et al. (2017) (see their Table 1) but using heat flux from ERA5 reanalysis, and our categorization agrees with Karpechko et al. (2017) except for the 01-05-2004 event: the 100hPa planetary wave heat flux does not reverse in ERA5 data, and hence we categorize this event as absorbing. The three most recent SSWs are all absorbing type in the first 11 days after SSW onset using the definition from Kodera et al. (2016) and Karpechko et al. (2017). Note that the Messori et al. (2022) and Kodera et al. (2016) definitions lead to large differences in which events are categorized as reflecting, and hence we separately analyze the possibility that absorptive events are more likely to be downward propagation for each definition.

We compare the downward propagation to the predictability of each SSW. We use two metrics of predictability: a hit rate metric and an absolute error metric. For the hit-rate metric, the following procedure is followed. An ensemble member is deemed "successful" if it simulates a SSW within ±3 days of its actual onset date. We then compute the earliest forecast lead day on which at least 50% of the ensemble members still successfully forecast the SSW for each model, and then compute the median predictability across models. This definition of a "success" follows Taguchi (2016), Taguchi (2020), D. I. Domeisen et al. (2020), Rao et al. (2019), Rao et al. (2020), and Chwat et al. (2022). In addition to this hit rate metric, we consider the absolute error, i.e. the absolute value of the difference between the ensemble mean predicted zonal wind at 60N, 10hPa and the actual zonal wind, averaged within ±1 day of the observed onset date. We then compute the earliest forecast lead day for each model in which the absolute error is less than 10m/s, and then compute the median predictability across models (Chwat et al., 2022).

3 Results

We begin by considering whether the models are able to predict the downward propagation of the SSW on December 15, 1998, the first event in the hindcast ensemble. Figure 1 (top left) contrasts the forecasted (grey, red, blue for different leads) U1060, Zcap500, and Zcap100 to that observed (black). Due to the relatively short forecast duration from these S2S models, and to match the methodology of Rao et al. (2020), U1060 is averaged from the SSW onset date to four days after, Zcap100 is averaged from the onset date to 14 days after onset, and Zcap500 is averaged from 5 days after onset to 19 days after onset. This event was classified as non-downward propagating by Karpechko et al. (2017), and consistent with this the polar cap averaged height at both 500hPa and 100hPa in ERA5 are only weakly above zero (black ×-es). Many of the initializations in days 2 to 9 before the SSW onset correctly predict both the severity of the deceleration of U1060 and the polar cap height anomaly; this is evident by how the gray circles envelop the reanalysis response in black. Initializations 10 to 17 and 18 to 25 days before the SSW are able to predict the sign of the U1060 and Zcap responses, however, they underestimate the amplitude. Hence, the forecasts for the SSW on December 15, 1998 converge on the "correct" solution as the lead time shortens, with the short lead forecasts successful.

For other SSW events, including the event on February 26, 1999, the modeling systems were less successful. This February 1999 event was strongly downward propagating in reality, however the models predict little downward propagation for Zcap at 100hPa or 500hPa, and the gray circles do not envelop the reanalysis response in black. The Zcap response is no better predicted for initializations 2 to 9 days before onset than 10 to 17 days before. While a few individual members initialized 10 to 17 and 18 to 25 before the SSW onset (red and blue circles) indicate quantitatively correct downward propagation, the models do not converge towards the "correct" solution for small forecast leads.

The remaining 11 SSWs shown in Figure 1 can be characterized as belonging to one of these two archetypes: the models struggle to capture the downward propagation and do not converge to the observed solution for SSWs on 01-18-2003 and 02-22-2008, while they converge towards the observed solution and envelop observations with the ensemble spread for the SSWs on 02-11-2001, 12-30-2001, 01-05-2004, 01-21-2006, 02-24-2007, 01-24-2009, 02-09-2010, and 01-06-2013. (The models also envelop the observations for the 03-20-2000 event, however, this event was weak by all three metrics, i.e. U1060, Zcap500, and Zcap100). We therefore characterize forecasts for the events on 02-26-1999, 01-18-2003, and 02-22-2008 as busts and the rest as relative successes. The latter two of these busts were non-downward propagating in reality, while the first was downward propagating. Hence, the downward impact for 75% of the SSWs (9 of 12 with strong anomalies) was predicted successfully in the S2S hindcasts. Note that Rao et al. (2020) find the real-time forecasts simulated reasonable downward impacts for the 2018 SSW and a relative lack of impacts for the 2019 SSW.

We now make this statement regarding prediction skill of the S2S models quantitative, by calculating the correlation coefficient between the ensemble mean and observed Zcap500 and Zcap100 across all events. These correlations are listed in Figure 1. There is a monotonic improvement in the ability of models to predict Zcap100 towards smaller leads, peaking at 0.82 at 2 to 9-day leads; hence two-thirds of the diversity in the Zcap100 response is well predicted before SSW onset. In contrast, the models struggle to predict which SSW event will have a strong impact on Zcap500, with a weaker improvement from 10 to 17 leads to 2 to 9 leads as compared to Z100. Note that we predict the observed Zcap500 response not using the model predicted Zcap500, but rather the model predicted Zcap100; the skill if we used Zcap500 from the models is even lower than that listed in Figure 1 (less than 0.3 even for day -2 to day -9 leads).

Part of this difficulty in capturing the tropospheric response could be that we have, thus far, considered the tropospheric impact only within the first nineteen days after SSW
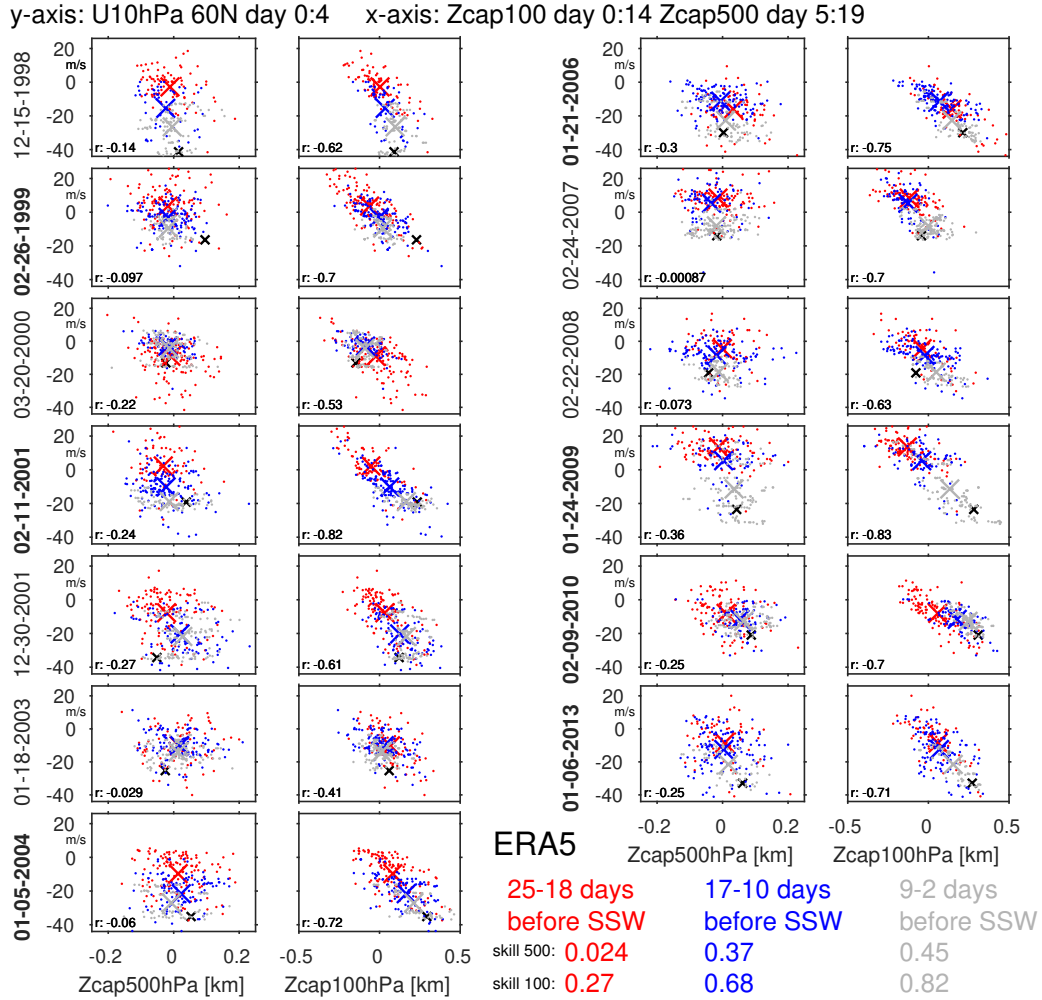
Figure 1. Scatterplot of the zonal mean zonal wind anomaly at 60°N/10 hPa (ordinates) versus the area-averaged polar $(70 - 90°\text{N})$ geopotential height anomaly (abscissas) for all ensemble members and all models. The wind is averaged from the SSW onset date to four days after, the polar geopotential height at 100hPa is averaged from the onset date to 14 days after onset, and the polar geopotential height at 500hPa is averaged from 5 days after onset to 19 days after onset. These lags match those of Rao et al. (2020); note that Rao et al. (2020) include similar figures but using the real-time forecasts preceding the 2018 and 2019 events, and similar figures have been created using the real-time forecasts preceding the 2021 SSW (not shown). The red dots are for initializations 25 to 18 days before SSW onset, and the blue and gray are for initializations 17 to 10 days and 9 to 2 days before SSW onset, respectively. The crosses indicate the ensemble mean for each of these lead times, and the black "×" is for the reanalysis. The correlations (r) between the zonal wind at 60°N and the polar cap geopotential height are included for each SSW event. SSW events classified as downward propagating by Karpechko et al. (2017) are indicated in bold.
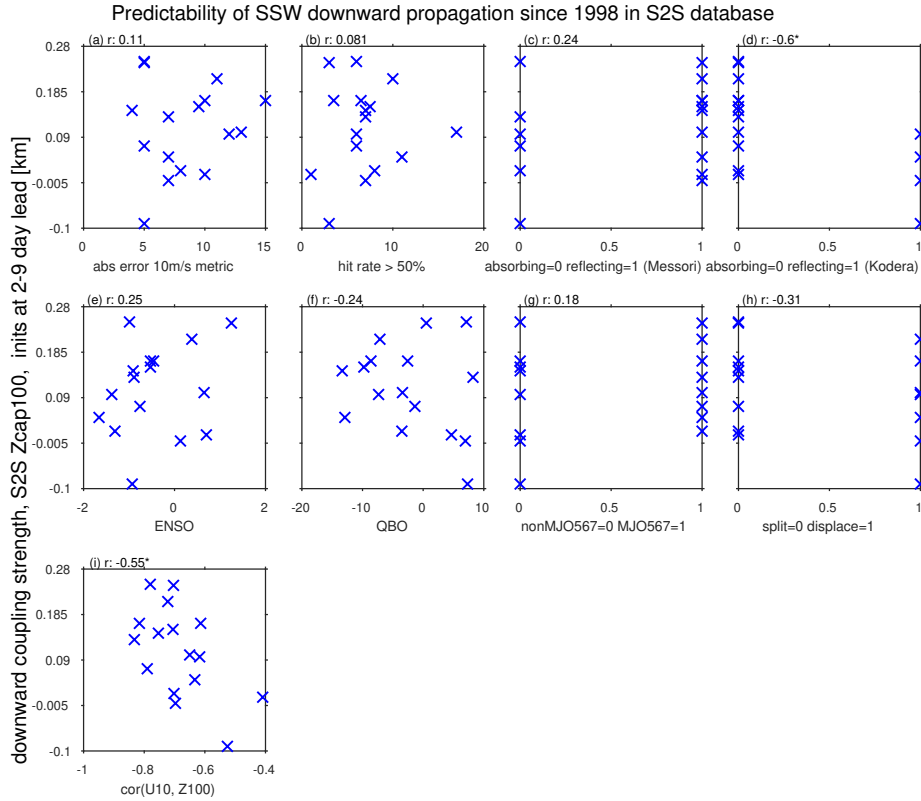
Figure 2. Scatterplots comparing the downward propagation as quantified by the multi-model mean (MME) Zcap100 (y-axis) to each of the following factors (x-axis): predictability of the SSW as given by the earliest forecast lead in which the median (a) absolute error of U1060 is less than 10m/s and (b) hit rate still exceeds 50%, across all models (Chwat et al., 2022); whether each SSW was absorbing or reflecting using the (c) Messori et al. (2022) definition and (d) Kodera et al. (2016) definition; (e) Niño3.4 index [Kelvin]; (f) Quasi-Biennial Oscillation [m/s]; (g) whether the event was preceded by Madden Julian Oscillation Phase 5, 6, or 7 of amplitude exceeding 1 in the two weeks before the event; (h) split versus displacement; (i) correlation between U1060 and polar cap height at 100hPa for each event (taken from Figure 1). Each of the 16 SSWs is indicated with an "x", and the correlation for each panel is indicated. Correlations exceeding 0.5 (in absolute value) allow rejecting a null hypothesis of no relationship at the 5% confidence level using a Student-t test and are indicated with a star next to the correlation.

onset due to the limited duration of the S2S hindcasts. The observed tropospheric impacts are sometimes strongest after 19 days. Indeed, if we predict the observed Zcap500 response averaged over days 5 to 35 (instead of 5 to 19) after SSW onset using initializations two to nine days before the SSW, correlations increase from 0.45 to 0.52. (The maximum skill arises if we use the model predicted Zcap100 response also averaged over days 5 to 35.) While it is remarkable that models become more skillful as we include longer lead times, this increase is marginal at best. Overall, the models successfully predict which SSWs have a strong downward impact on lower stratospheric polar cap height, though only 25% of the inter-event spread in the tropospheric impact is predicted before the SSW onset.

A reliable subseasonal forecast depends not only on identifying which SSW will have a strong downward impact but also on predicting the SSW as far in advance as is pos-
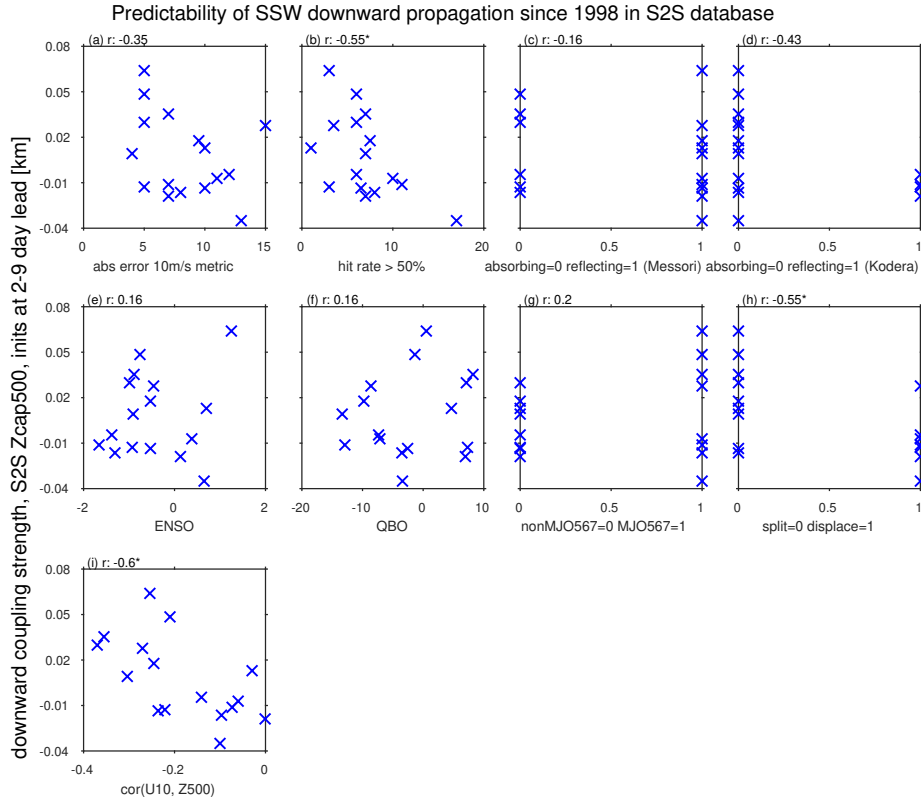
Figure 3. As in Figure 2 but replacing the y-axis with the MME Zcap500.

sible in the first place. Chwat et al. (2022) recently evaluated the predictability of these 16 SSWs in the S2S hindcasts and reforecasts, and found that predictability ranged from less than five days to nearly twenty days depending on the SSW event. Figures 2ab-3ab contrast the median predictability of each SSW to the magnitude of the Zcap100 and Zcap500 response as predicted by the S2S models. We consider both metrics of SSW predictability introduced in Section 2, and we also include the three SSWs since 2018 in this analysis to maximize the sample size. There is no relationship between predictability and observed downward propagation to 100hPa (Figures 2ab), and if anything predictability is negatively correlated with downward propagation to 500hPa (Figure 3ab). That is, SSWs that were harder to predict had a stronger downward impact at 500hPa, and this effect is statistically significant at the 95% level. Results are generally similar if we use the observed downward propagation rather than that simulated by the S2S models (supplemental Figures 1-2).

Next, we revisit possible factors that have previously been proposed to encourage stronger propagation (see Section 1). We evaluate whether these factors help account for the relative strength of downward propagation in reanalysis data, and then consider whether these factors can encourage strong downward propagation in the S2S models. We include the three SSWs since 2018 in this analysis to maximize the sample size.

Previous work has suggested that reflecting SSWs tend to have a weaker zonal mean surface impact than absorbing SSWs. Two alternate indices have been used in the literature to quantify the absorption/reflectivity of SSWs (see Section 2), and we consider both in Figures 2cd-3cd for downward propagation in the models and supplemental Figures 1cd/2cd for observed downward propagation. Observed downward propagation to 500hPa is stronger for absorbing events as defined by either definition, though downward

propagation to 100hPa is stronger only for the Kodera definition. The S2S models also indicate stronger downward propagation for the Kodera absorbing events, while Messori absorbing vs. reflecting events show no significant difference in downward propagation. Note that we used a polar cap averaged height index to track downward propagation, and it is conceivable that the impact of Messori absorbing vs. reflecting events is limited to certain sectors (e.g. North America). Future work should consider this possibility.

I. White et al. (2019) found in a large ensemble of chemistry-climate model simulations that a stronger pulse of upward wave forcing that precedes the SSW tends to encourage downward propagation, however, at least 30 events of each type are needed before the effect becomes statistically robust. We consider the relationship between downward propagation and three phenomena known to enhance upward wave flux into the vortex region in Figures 2efg-3efg and Supplemental Figures 1-2efg. While El Niño, easterly QBO, and MJO phase 5/6/7 events all are associated with a slight increase in the downward propagation to 100hPa both in ERA5 and in the S2S models, the relationship is not statistically significant. Stronger downward propagation to 500hPa is both simulated and observed for SSWs preceded by MJO phase 5/6/7, however for ENSO and the QBO there is little consistency between the S2S models and ERA5. None of these connections are statistically significant however, consistent with I. White et al. (2019) who find that 16 SSWs (i.e., the sample size available) is a factor of 4 too small for such a signal to emerge from the noise.

Split SSWs are known to have a stronger near-term surface impact than displacement SSWs (Mitchell et al., 2013; I. P. White et al., 2021), and this relationship is both simulated and observed. Namely, for both Zcap100 and Zcap500, the SSW downward propagation is significantly stronger for splits (Figures 2h-3h).

Rao et al. (2020) found that downward propagation for the 2018 and 2019 SSWs was more strongly associated with the magnitude of the coupling between U1060 and Zcap than with the wave morphology. We consider this possibility in Figures 2h-3h, which contrasts the coupling strength between U1060 and Zcap (listed on each panel of Figure 1) with the Zcap response. As expected, the Zcap response at both 100hPa and 500hPa is significantly stronger for SSWs in which U1060 and Zcap are more tightly coupled. This relationship is somewhat stronger than the relationship with vortex morphology and hence is also consistent with Rao et al. (2020).

Overall, we find support for previously proposed factors that have been linked to the strength of downward propagation. Previous work has found evidence for these factors in free-running climate simulations or for a limited selection of observed SSWs. Here, we expand on this previous work and find that these factors are relevant for predicting downward propagation in the S2S model hindcasts as well.

While the goal of this work is not to assess the skill of individual S2S models, there are some interesting differences across models. Table 1 summarizes each model's ability to capture SSW downward propagation for the 11 SSWs common to all models for lead times of 2 to 9 days before SSW onset. The two low-top models (BoM and CMA) struggle to capture the full magnitude of the observed signal even in the stratosphere. In contrast, the high-top models all simulate a reasonable downward signal at least to 100hPa. It is notable that the magnitude of the Zcap100 and U1060 responses are correlated across models, such that the low-top models simulate a too-weak response for both. An alternate method to quantify the magnitude of downward coupling is to compute the correlation between U1060 and Zcap100 and Zcap500, and also between Zcap100 and Zcap500, for each model. Table 1 demonstrates a wide spread in the connection between Zcap100 and Zcap500, and also between Zcap100 and U1060: in KMA and NCEP there is essentially no relationship between the U1060 and Zcap500 responses, while in others there is strong coupling. Future work should focus on why coupling strength between

the stratosphere and the troposphere differs across models, which will lead to further insights on the dynamics of stratosphere - troposphere coupling.

4 Discussion and Conclusion

The occurrence of a sudden stratospheric warming (SSW) opens a window of opportunity for subseasonal predictability in much of the extratropics (Sigmond et al., 2013; D. I. Domeisen et al., 2020; D. I. V. Domeisen, Butler, et al., 2020). Not all SSWs are followed by the canonical impact of a negative NAM, however, and forecast skill and reliability would be enhanced if it could be predicted in advance which SSWs propagate downward versus which ones do not. We revisit this question using hindcasts and real-time forecasts provided by operational subseasonal forecasting models.

The S2S models successfully predict two to nine days before SSW onset whether a SSW will propagate downward to the lower stratosphere for 75% of the SSWs considered in this paper. Further, these models can predict $\sim$ 2/3 of the inter-event spread in the polar cap height response at 100hPa. Hence the models are largely able to predict downward propagation to the lower stratosphere, especially for forecast leads within 10 days of the SSW onset. On the other hand, the models are less successful at predicting the tropospheric impacts, though they still account for $\sim$ 1/4 of the inter-event spread in the polar cap height response at 500hPa.

While it would be convenient for planning purposes if the most predictable SSWs were also the ones with the strongest downward impacts, this is not the case. There is no relationship between the downward propagation of a SSW to 100hPa to whether the SSW event itself is predictable. Further, the SSW events with a strong tropospheric imprint tend to be less predictable than average. This (unfortunate) confluence is somewhat to be expected from previous work: displacement events are generally more predictable (Taguchi, 2018; D. I. Domeisen et al., 2020; Chwat et al., 2022), but splits have a stronger near-term downward impact (Mitchell et al., 2013; I. P. White et al., 2021).

Downward propagation in the S2S models is stronger for absorbing and split SSWs, consistent with previous work that has analyzed observational downward propagation. Downward propagation is also significantly enhanced for members which better capture the U1060 response (consistent with Rao et al., 2020). SSWs and models with a tighter relationship between U1060 and polar cap height also simulate stronger downward propagation. Ongoing work is aimed at a process-based diagnosis of stratosphere-troposphere coupling processes in these models, with the hope of pinpointing areas for improvement.

(A) summary of Zcap for each model

event	Zcap500	Zcap100	U1060
ERA5	0.014	0.13	-21.99
NCEP	0.007	0.11	-20.62
KMA	-0.017	0.08	-18.86
CMA	-0.004	0.08	-16.78
CNRM	0.017	0.15	-22.89
ECMWF2019	0.013	0.13	-19.55
UKMO2020	0.000	0.11	-20.76
BOM	0.002	0.06	-10.23

(B) summary of correlation for each model

event	Zcap500	Zcap100	Zcap100500
NCEP	0.01	-0.60	0.46
KMA	-0.01	-0.56	0.57
CMA	-0.21	-0.68	0.63
CNRM	-0.26	-0.71	0.60
ECMWF2019	-0.16	-0.70	0.57
UKMO2020	-0.08	-0.63	0.55
BOM	-0.20	-0.66	0.70

Table 1. (A) Mean response for the 11 SSWs in the common period (1999-2010) for each model for (left) Zcap at 500hPa; (middle) Zcap at 100hPa; (right) U1060. (B) Mean correlation for the 11 SSWs in the common period (1999-2010) for each model for the (left) correlation between U1060 and Zcap 500hPa; (middle) correlation between U1060 and Zcap 100hPa; (right) correlation between Zcap 500hPa and Zcap 100hPa.

5 Open Research

The original S2S database is hosted at ECMWF as an extension of the TIGGE database, and can be downloaded from the ECMWF server `http://apps.ecmwf.int/datasets/data/s2s/levtype=sfc/type=cf/`. The QBO data was downloaded from the NCEP website `https://www.cpc.ncep.noaa.gov/data/indices/qbo.u50.index`. The real time multivariate index of Wheeler and Hendon (2004) was downloaded from the BoM website (`http://www.bom.gov.au/climate/mjo/graphics/rmm.74toRealtime.txt`).

References

Afargan-Gerstman, H., Büeler, D., Wulff, C. O., Sprenger, M., & Domeisen, D. I. (2024). Stratospheric influence on the winter North Atlantic storm track in subseasonal reforecasts. *Weather and Climate Dynamics*, *5*, 231–249.

Afargan-Gerstman, H., & Domeisen, D. I. (2020). Pacific modulation of the North Atlantic storm track response to sudden stratospheric warming events. *Geophysical Research Letters*, *47*(2), e2019GL085007.

Afargan-Gerstman, H., Jiménez-Esteve, B., & Domeisen, D. I. (2022). On the relative importance of stratospheric and tropospheric drivers for the North Atlantic jet response to sudden stratospheric warming events. *Journal of Climate*, *35*(19), 6453–6467.

Afargan-Gerstman, H., Polkova, I., Papritz, L., Ruggieri, P., King, M. P., Athanasiadis, P. J., ... Domeisen, D. I. (2020). Stratospheric influence on North Atlantic marine cold air outbreaks following sudden stratospheric warming events. *Weather and Climate Dynamics*, *1*(2), 541.

Baldwin, M. P., Ayarzagüena, B., Birner, T., Butchart, N., Butler, A. H., Charlton-Perez, A. J., ... others (2021). Sudden stratospheric warmings. *Reviews of Geophysics*, *59*(1), e2020RG000708.

Baldwin, M. P., Stephenson, D. B., Thompson, D. W. J., Dunkerton, T. J., Charlton, A. J., & O'Neill, A. (2003). Stratospheric memory and skill of extended-range weather forecasts. *Science*, *301*. doi: 10.1126/science.1087143

Black, R. X., & McDaniel, B. A. (2004). Diagnostic case studies of the northern annular mode. *Journal of Climate*, *17*(20), 3990 - 4004. Retrieved from `https://journals.ametsoc.org/view/journals/clim/17/20/1520-0442_2004_017_3990_dcsotn_2.0.co_2.xml` doi: https://doi.org/10.1175/1520-0442(2004)017⟨3990:DCSOTN⟩2.0.CO;2

Butler, A. H., Seidel, D. J., Hardiman, S. C., Butchart, N., Birner, T., & Match, A. (2015). Defining sudden stratospheric warmings. *Bulletin of the American Meteorological Society*, *96*(11), 1913–1928.

Butler, A. H., Sjoberg, J. P., Seidel, D. J., & Rosenlof, K. H. (2017). A sudden stratospheric warming compendium. *Earth System Science Data*, *9*(1), 63–76.

Charlton, A. J., & Polvani, L. M. (2007). A New Look at Stratospheric Sudden Warmings. Part I: Climatology and Modeling Benchmarks. *Journal of Climate*, *20*, 449-+. doi: 10.1175/JCLI3996.1

Chwat, D., Garfinkel, C. I., Chen, W., & Rao, J. (2022). Which sudden stratospheric warming events are most predictable? *Journal of Geophysical Research: Atmospheres*, *127*(18), e2022JD037521. Retrieved from `https://agupubs.onlinelibrary.wiley.com/doi/abs/10.1029/2022JD037521` (e2022JD037521 2022JD037521) doi: https://doi.org/10.1029/2022JD037521

Cohen, J., Agel, L., Barlow, M., Garfinkel, C. I., & White, I. (2021). Linking arctic variability and change with extreme winter weather in the united states. *Science*, *373*(6559), 1116-1121. Retrieved from `https://www.science.org/doi/abs/10.1126/science.abi9167` doi: 10.1126/science.abi9167

Cohen, J., & Jones, J. (2011). Tropospheric Precursors and Stratospheric Warmings. *Journal of Climate*, *24*. doi: 10.1175/2011JCLI4160.1

Domeisen, D. I. (2019). Estimating the frequency of sudden stratospheric warming events from surface observations of the north atlantic oscillation. *Journal of Geophysical Research: Atmospheres*, *124*(6), 3180–3194.

Domeisen, D. I., Butler, A. H., Charlton-Perez, A. J., Ayarzaguena, B., Baldwin, M. P., Dunn-Sigouin, E., . . . Taguchi, M. (2020). The role of the stratosphere in sub-seasonal to seasonal prediction: 1. Predictability of the stratosphere. *Journal of Geophysical Research: Atmospheres*, *125*(2), e2019JD030920. Retrieved from `https://agupubs.onlinelibrary.wiley.com/doi/abs/10.1029/2019JD030920` doi: https://doi.org/10.1029/2019JD030920

Domeisen, D. I., White, C. J., Afargan-Gerstman, H., Muñoz, Á. G., Janiga, M. A., Vitart, F., . . . others (2022). Advances in the subseasonal prediction of extreme events: relevant case studies across the globe. *Bulletin of the American Meteorological Society*, *103*(6), E1473–E1501.

Domeisen, D. I. V., Butler, A. H., Charlton-Perez, A. J., Ayarzaguena, B., Baldwin, M. P., Dunn-Sigouin, E., . . . Taguchi, M. (2020). The role of the stratosphere in sub-seasonal to seasonal prediction: 2. Predictability arising from stratosphere-troposphere coupling. *Journal of Geophysical Research: Atmospheres*, *125*(2), e2019JD030923. Retrieved from `https://agupubs.onlinelibrary.wiley.com/doi/abs/10.1029/2019JD030923` doi: https://doi.org/10.1029/2019JD030923

Domeisen, D. I. V., Grams, C. M., & Papritz, L. (2020). The role of North Atlantic–European weather regimes in the surface impact of sudden stratospheric warming events. *Weather and Climate Dynamics*, *1*(2), 373–388. doi: 10.5194/wcd-1-373-2020

Garfinkel, C. I., Feldstein, S. B., Waugh, D. W., Yoo, C., & Lee, S. (2012). Observed Connection between Stratospheric Sudden Warmings and the Madden-Julian Oscillation. *Geophys. Res. Lett.*, *39*, L18807. doi: http://dx.doi.org/10.1029/2012GL053144

Garfinkel, C. I., Son, S.-W., Song, K., Aquila, V., & Oman, L. D. (2017). Stratospheric variability contributed to and sustained the recent hiatus in eurasian winter warming. *Geophysical research letters*, *44*(1), 374–382. doi: 10.1002/2016GL072035

Hersbach, H., Bell, B., Berrisford, P., Hirahara, S., Horányi, A., Muñoz-Sabater, J., . . . others (2020). The era5 global reanalysis. *Quarterly Journal of the Royal Meteorological Society*, *146*(730), 1999–2049.

Hitchcock, P., Shepherd, T. G., & Manney, G. L. (2013). Statistical characterization of arctic polar-night jet oscillation events. *Journal of Climate*, *26*(6), 2096–2116.

Hitchcock, P., & Simpson, I. R. (2014). The downward influence of stratospheric sudden warmings. *Journal of the Atmospheric Sciences*, *71*(10), 3856–3876.

Huang, B., Thorne, P. W., Banzon, V. F., Boyer, T., Chepurin, G., Lawrimore, J. H., . . . Zhang, H.-M. (2017). Extended reconstructed sea surface temperature, version 5 (ersstv5): upgrades, validations, and intercomparisons. *Journal of Climate*, *30*(20), 8179–8205.

Jucker, M. (2016). Are sudden stratospheric warmings generic? insights from an idealized gcm. *Journal of the Atmospheric Sciences*, *73*(12), 5061–5080.

Karpechko, A. Y., Charlton-Perez, A., Balmaseda, M., Tyrrell, N., & Vitart, F. (2018). Predicting sudden stratospheric warming 2018 and its climate impacts with a multimodel ensemble. *Geophysical Research Letters*, *45*(24), 13–538.

Karpechko, A. Y., Hitchcock, P., Peters, D. H., & Schneidereit, A. (2017). Predictability of downward propagation of major sudden stratospheric warmings. *Quarterly Journal of the Royal Meteorological Society*, *143*(704), 1459–1470.

Kodera, K., Mukougawa, H., Maury, P., Ueda, M., & Claud, C. (2016). Absorbing and reflecting sudden stratospheric warming events and their relationship with tropospheric circulation. *Journal of Geophysical Research: Atmospheres*, *121*(1), 80–94. doi: 10.1002/2015JD023359

Kolstad, E. W., Breiteig, T., & Scaife, A. A. (2010). The association between stratospheric weak polar vortex events and cold air outbreaks in the northern hemisphere. *Quarterly Journal of the Royal Meteorological Society*, *136*(649), 886–893.

Kolstad, E. W., Wulff, C. O., Domeisen, D. I. V., & Woollings, T. (2020). Tracing North Atlantic Oscillation Forecast Errors to Stratospheric Origins. *Journal of Climate*, *33*(21), 9145–9157. doi: 10.1175/JCLI-D-20-0270.1

Kretschmer, M., Coumou, D., Agel, L., Barlow, M., Tziperman, E., & Cohen, J. (2018). More-persistent weak stratospheric polar vortex states linked to cold extremes. *Bulletin of the American Meteorological Society*, *99*(1), 49-60. doi: 10.1175/BAMS-D-16-0259.1

Lehtonen, I., & Karpechko, A. Y. (2016). Observed and modeled tropospheric cold anomalies associated with sudden stratospheric warmings. *Journal of Geophysical Research: Atmospheres*, *121*(4), 1591–1610. Retrieved from http://dx.doi.org/10.1002/2015JD023860 (2015JD023860) doi: 10.1002/2015JD023860

Maycock, A. C., & Hitchcock, P. (2015). Do split and displacement sudden stratospheric warmings have different annular mode signatures? *Geophysical Research Letters*, *42*(24).

Messori, G., Kretschmer, M., Lee, S. H., & Wendt, V. (2022). Stratospheric downward wave reflection events modulate north american weather regimes and cold spells. *Weather and Climate Dynamics*, *3*(4), 1215–1236.

Mitchell, D., Gray, L., Anstey, J., Baldwin, M., & Charlton-Perez, A. (2013). The influence of stratospheric vortex displacements and splits on surface climate. *J. Clim.*, *26*(8), 2668-2682.

Rao, J., Garfinkel, C. I., Chen, H., & White, I. P. (2019). The 2019 new year stratospheric sudden warming and its real-time predictions in multiple s2s models. *Journal of Geophysical Research: Atmospheres*, *124*. doi: 10.1029/2019JD030826

Rao, J., Garfinkel, C. I., & White, I. P. (2020). Predicting the Downward and Surface Influence of the February 2018 and January 2019 Sudden Stratospheric Warming Events in Subseasonal to Seasonal (S2S) Models. *Journal of Geophysical Research: Atmospheres*, *125*(2), e2019JD031919. Retrieved from https://agupubs.onlinelibrary.wiley.com/doi/abs/10.1029/2019JD031919 doi: https://doi.org/10.1029/2019JD031919

Rao, J., Garfinkel, C. I., Wu, T., Lu, Y., Lu, Q., & Liang, Z. (2021). The January 2021 Sudden Stratospheric Warming and Its Prediction in Subseasonal to Seasonal Models. *Journal of Geophysical Research: Atmospheres*, *126*(21), e2021JD035057.

Runde, T., Dameris, M., Garny, H., & Kinnison, D. (2016). Classification of stratospheric extreme events according to their downward propagation to the troposphere. *Geophysical Research Letters*, *43*(12), 6665–6672.

Schoeberl, M. R. (1978). Stratospheric warmings: Observations and theory. *Rev. of*

Geophys. and Space Physics.

Sigmond, M., Scinocca, J., Kharin, V., & Shepherd, T. (2013). Enhanced seasonal forecast skill following stratospheric sudden warmings. *Nature Geoscience*, *6*(2), 98–102. doi: 10.1038/ngeo1698

Taguchi, M. (2016). Connection of predictability of major stratospheric sudden warmings to polar vortex geometry. *Atmospheric Science Letters*, *17*(1), 33-38. Retrieved from `https://rmets.onlinelibrary.wiley.com/doi/abs/10.1002/asl.595` doi: https://doi.org/10.1002/asl.595

Taguchi, M. (2018). Comparison of subseasonal-to-seasonal model forecasts for major stratospheric sudden warmings. *Journal of Geophysical Research: Atmospheres*, *123*(18), 10231-10247. Retrieved from `https://agupubs.onlinelibrary.wiley.com/doi/abs/10.1029/2018JD028755` doi: https://doi.org/10.1029/2018JD028755

Taguchi, M. (2020). Verification of subseasonal-to-seasonal forecasts for major stratospheric sudden warmings in northern winter from 1998/99 to 2012/13. *Advances in Atmospheric Sciences*, *37*(3), 250–258.

Thompson, D. W. J., Baldwin, M. P., & Wallace, J. M. (2002). Stratospheric Connection to Northern Hemisphere Wintertime Weather: Implications for Prediction. *J. Clim.*, *15*, 1421–1428. doi: 10.1175/1520-0442(2002)015

Tripathi, O. P., Baldwin, M., Charlton-Perez, A., Charron, M., Cheung, J. C., Eckermann, S. D., ... others (2016). Examining the predictability of the stratospheric sudden warming of january 2013 using multiple nwp systems. *Monthly Weather Review*, *144*(5), 1935–1960.

Tripathi, O. P., Baldwin, M., Charlton-Perez, A., Charron, M., Eckermann, S. D., Gerber, E., ... Son, S. W. (2015). The predictability of the extra-tropical stratosphere on monthly timescales and its impact on the skill of tropospheric forecasts. *Quarterly Journal of the Royal Meteorological Society*, *141*. doi: 10.1002/qj.2432

Vitart, F., Ardilouze, C., Bonet, A., Brookshaw, A., Chen, M., Codorean, C., ... others (2017). The sub-seasonal to seasonal prediction (s2s) project database. *Bulletin of the American Meteorological Society*. doi: 10.1175/BAMS-D-16-0017.1

Wheeler, M. C., & Hendon, H. H. (2004). An All-Season Real-Time Multivariate MJO Index: Development of an Index for Monitoring and Prediction. *Monthly Weather Review*, *132*, 1917. doi: 10.1175/1520-0493(2004)132⟨1917:AARMMI⟩2.0.CO;2

White, I., Garfinkel, C. I., Gerber, E. P., Jucker, M., Aquila, V., & Oman, L. D. (2019). The downward influence of sudden stratospheric warmings: Association with tropospheric precursors. *Journal of Climate*, *32*(1), 85-108. doi: 10.1175/JCLI-D-18-0053.1

White, I. P., Garfinkel, C. I., Cohen, J., Jucker, M., & Rao, J. (2021). The impact of split and displacement sudden stratospheric warmings on the troposphere. *Journal of Geophysical Research: Atmospheres*, *126*(8), e2020JD033989. Retrieved from `https://agupubs.onlinelibrary.wiley.com/doi/abs/10.1029/2020JD033989` (e2020JD033989 2020JD033989) doi: https://doi.org/10.1029/2020JD033989

Figure 1.

y-axis: U10hPa 60N day 0:4   x-axis: Zcap100 day 0:14 Zcap500 day 5:19

Left panels (top to bottom): 12-15-1998, **02-26-1999**, 03-20-2000, **02-11-2001**, 12-30-2001, 01-18-2003, **01-05-2004**

Right panels (top to bottom): **01-21-2006**, 02-24-2007, 02-22-2008, **01-24-2009**, 02-09-2010, **01-06-2013**

Left column x-axis labels: Zcap500hPa [km], Zcap100hPa [km]
Right column x-axis labels: Zcap500hPa [km], Zcap100hPa [km]

ERA5

	25-18 days before SSW	17-10 days before SSW	9-2 days before SSW
skill 500:	0.024	0.37	0.45
skill 100:	0.27	0.68	0.82

r values (left column):
- 12-15-1998: r: -0.14 ; r: -0.62
- 02-26-1999: r: -0.097 ; r: -0.7
- 03-20-2000: r: -0.22 ; r: -0.53
- 02-11-2001: r: -0.24 ; r: -0.82
- 12-30-2001: r: -0.27 ; r: -0.61
- 01-18-2003: r: -0.029 ; r: -0.41
- 01-05-2004: r: -0.06 ; r: -0.72

r values (right column):
- 01-21-2006: r: -0.3 ; r: -0.75
- 02-24-2007: r: -0.00087 ; r: -0.7
- 02-22-2008: r: -0.073 ; r: -0.63
- 01-24-2009: r: -0.36 ; r: -0.83
- 02-09-2010: r: -0.25 ; r: -0.7
- 01-06-2013: r: -0.25 ; r: -0.71

Figure 2.

Predictability of SSW downward propagation since 1998 in S2S database
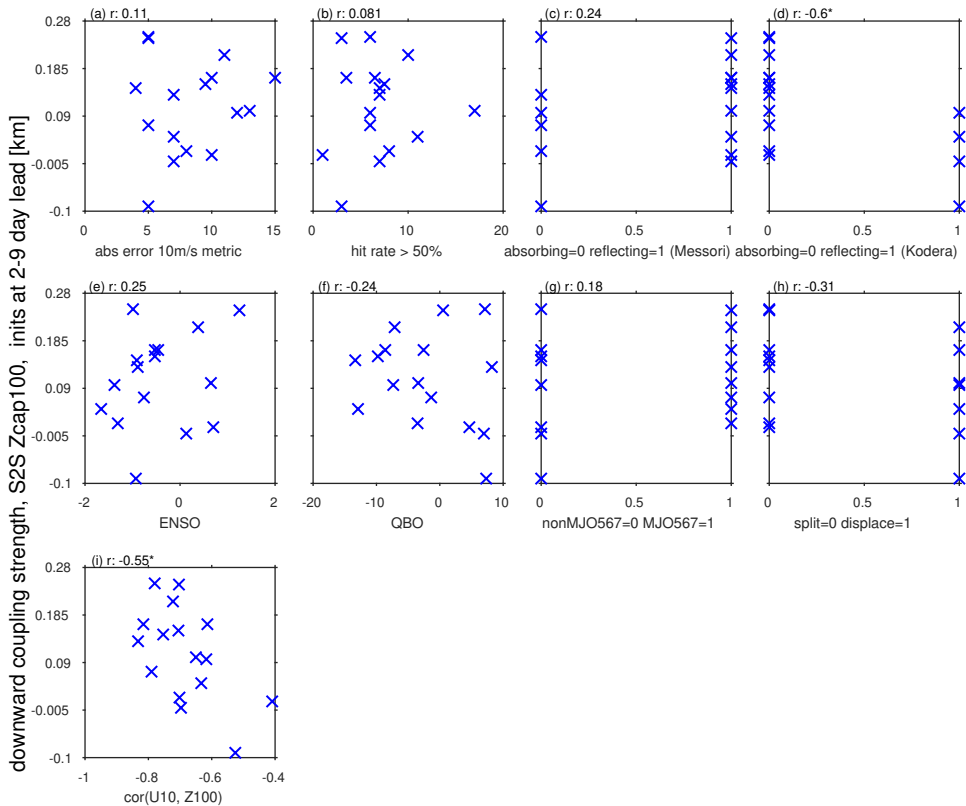
Figure 3.

Predictability of SSW downward propagation since 1998 in S2S database